Inorganic Chemistry

Article

pubs.acs.org/IC

Oxo-Bridged Dinuclear Chromium(III) Complexes: Correlation between the Optical and Magnetic Properties and the Basicity of the Oxo Bridge

Thorbjørn J. Morsing, Jesper Bendix, Høgni Weihe, and Anders Døssing*

Department of Chemistry, University of Copenhagen, Universitetsparken 5, DK-2100 Copenhagen, Denmark

Supporting Information

ABSTRACT: The synthesis and X-ray structure of a new member of the series of oxo-bridged, dinuclear chromium(III) complexes, the methyl isocyanide complex $[(CH_3NC)_5CrOCr(CNCH_3)_5](PF_6)_4{\cdot}2CH_3CN$, is reported. This constitutes only the third oxo-bridged, dinuclear chromium(III) complex with a homoleptic auxillay ligand sphere. Experimentally, the system shows unshifted narrow nuclear magnetic resonance (NMR) spectra that are consistent with calculations using broken symmetry density functional theory (DFT), which suggests it to be the strongest coupled, dinuclear chromium(III) complex known. Furthermore, we report the crystal structure and computed magnetic properties for $[(bpy)_2(SCN)CrOCr(NCS)(bpy)_2](ClO_4)_2{\cdot}2H_2O$ (bpy = 2,2′-bipyridine), which differs from other reported oxo-bridged species by featuring a bent $CrOCr^{4+}$ core. We also interpret the spectacular 10-orders-of-magnitude variation in acid dissociation constant of the bridging hydroxo ligand in mono hydroxo-bridged dinuclear chromium(III) complexes, in terms of a valence bond model parametrized by metal-to-metal charge transfer (MMCT) and ligand-to-metal charge transfer (LMCT) energies.

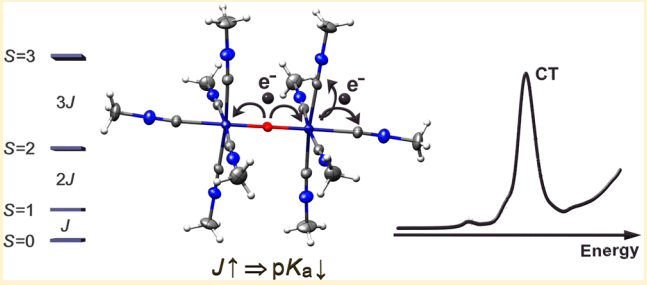

INTRODUCTION

The complex ion $[(NH_3)_5CrOCr(NH_3)_5]^{4+}$ (**1**), traditionally referred to as "basic rhodo", was first synthesized by Jørgensen in 1882,[1] and for a long time, it was the only known oxo-bridged dinuclear chromium(III) complex with a homoleptic outer ligand sphere. Since then, many oxo-bridged dinuclear chromium(III) complexes have been synthesized. Selected complexes are listed in Table 1, with the most recent being the acetonitrile analogue $[(CH_3CN)_5CrOCr(NCCH_3)_5]^{4+}$ (**10**).[2]

The magnetic exchange coupling between the two chromium(III) centers has been measured by various techniques, in most cases by susceptibility measurements. The exchange coupling has also been determined by high field and frequency electron paramagnetic resonance,[13] but it was successful because the coupling was smaller in magnitude than for the oxo-bridged systems here. Therefore, we are limited to magnetic susceptibility measurements. Antiferromagnetic coupling in **1** was recognized early to be very strong and quantified as J = 450 cm^{-1} ($\hat{H} = JS_1{\cdot}S_2$),[3] while the value in **10** was determined to be, via susceptibility measurements, J = 650 cm^{-1},[11] which is the highest reported for an oxo-bridged dinuclear chromium(III) complex to date. We have previously demonstrated that density functional theory (DFT) is able to reproduce, within 10%, the experimental values of J for a range of complexes of this type,[11] with the calculated values of J in **1** and **10** being 441 and 685 cm^{-1}, respectively.

In constrast to **1**, the acetonitrile analogue (**10**) was found to be nonbasic, with the pK_a value for the corresponding hydroxo-bridged species (see eq 1) being below −2,[12] compared to 7.6 for the protonated form of **1**, the "acid rhodo".[4]

$$[L_5Cr(OH)CrL_5]^{5+} \rightleftarrows [L_5CrOCrL_5]^{4+} + H^+ \qquad K_a \tag{1}$$

It is well-established that the acidity of coordinated water molecules depends on the chemical nature of the remaining ligand sphere, because of differences in hydration energy between the protonated and the unprotonated form. Table 2 demonstrates this by listing the acidity of a series of mononuclear, tricationic, aqua complexes of chromium(III). However, it is seen that the values of pK_{a1} spans a range of only two pK_a units, depending on the nature of the ligands; this variation is not at all comparable to the huge difference between **1** and **10**. In the present work, we have synthesized a new basic rhodo analogue with methyl isocyanide as the auxiliary ligand, $[(CH_3NC)_5CrOCr(CNCH_3)_5]^{4+}$ (**11**), in which the antiferromagnetic coupling is even stronger than in **10** and the basicity of the oxo bridge is still lower than in **10**. Earlier, we suggested a correlation between the π acidity of the auxiliary coligands and the values of J in terms of nephelauxetism.[11,12] Moreover, Holwerda, on the basis of a series of dinuclear, oxobridged polypyridyl complexes of chromium(III), has tentatively suggested a correlation between the π acidity of the auxiliary ligands, the value of J, and the

Received: November 8, 2013
Published: March 5, 2014

   dx.doi.org/10.1021/ic4027927 | *Inorg. Chem.* 2014, 53, 2996−3003

Table 1. Oxo-bridged Dinuclear Chromium(III) Complexes for Which the Acid/Base Properties Have Been Investigated; Acid Dissociation Constants for the Hydroxo-bridged Complexes (pK_a) are Collected, along with Available Cr−O Bond Distances (r), Experimental and Calculated Values of the Exchange Coupling Constants (Triplet Energy, J), and Cr ← O Charge-Transfer Energies (E_{CT})[a]

i	oxo-bridged complex	pK_a	r (Å)	J(exp) (cm^{-1})	J(calc) (cm^{-1})[b]	E_{CT} (cm^{-1})[c]	ref
1	$[Cr(NH_3)_5]_2O^{4+}$	7.63	1.803	450	441	36200	3−6
2	$[Cr(tpa)N_3]_2O^{2+}$	4.25					7
3	$[Cr(tpa)(NCO)]_2O^{2+}$	4.09					7
4	$[Cr(tpa)Cl]_2O^{2+}$	4.01					7, 8
5	$[Cr(tpa)(NCS)]_2O^{2+}$	2.05	1.8001	510	487		8, 9
6	$[Cr(tpa)(NCSe)]_2O^{2+}$	1.48					8
7	$[Cr(tpa)(CN)]_2O^{2+}$	0.64		580			7
8	$[Cr(bpy)_2(NCS)]_2O^{2+}$	∼0	1.799[d]	494	468		10, this work
9	$[Cr(phen)_2(NCS)]_2O^{2+}$	∼0		542			10
10	$[Cr(NCCH_3)_5]_2O^{4+}$	less than −2[e]	1.7556	650[f]	685	31800	2, 11, 12
11	$[Cr(CNCH_3)_5]_2O^{4+}$	much less than −2[g]	1.7712		825	29150	this work

[a]Abbreviations used: tpa = tris(2-pyridylmethyl)amine; bpy = 2,2′-bipyridine; phen = 1,10-phenanthroline. [b]This value is obtained using broken symmetry DFT calculations with a level of theory known to accurately reproduce exchange coupling constants for this particular type of dinuclear chromium(III) complexes.[11] [c]The position of this absorption band cannot be determined for the tpa, bpy, and phen complexes, because these ligands have intense absorption in this energy region. [d]Δ,Δ/Λ,Λ isomer. [e]Value is estimated from absorption spectra recorded in 1 M perchloric acid wherein the spectrum showed no trace of hydroxo-bridged complex. [f]Absorption spectra of the BF_4^- salt in frozen solution indicate a larger value. [g]Value is estimated from absorption spectra recorded in concentrated perchloric acid wherein the spectrum of the dinuclear complex did not change.

Table 2. Values for the First Acid Dissociation Constants (pK_{a1}) for Selected Aqua Complexes of Chromium(III)[a]

complex	pK_{a1}	ref
$[Cr(NH_3)_5(OH_2)]^{3+}$	5.18	14
trans-$[Cr(NH_3)_4(OH_2)_2]^{3+}$	4.38	15
cis-$[Cr(NH_3)_4(OH_2)_2]^{3+}$	4.96	15
trans-$[Cr(en)_2(OH_2)_2]^{3+}$	4.11	15
cis-$[Cr(en)_2(OH_2)_2]^{3+}$	4.75	15
cis-$[Cr(phen)_2(OH_2)_2]^{3+}$	3.4	16
fac-$[Cr(NH_3)_3(OH_2)_3]^{3+}$	5.00	17
mer-$[Cr(NH_3)_3(OH_2)_3]^{3+}$	4.46	17
fac-$[Cr(NH_2CH_3)_3(OH_2)_3]^{3+}$	4.78	18
mer-$[Cr(NH_2CH_3)_3(OH_2)_3]^{3+}$	4.06	18
$[Cr(tacn)(OH_2)_3]^{3+}$	4.57	19
$[Cr(tame)(OH_2)_3]^{3+}$	4.93	20
$[Cr(Me_3\text{-}tame)(OH_2)_3]^{3+}$	4.78	21
$[Cr(OH_2)_6]^{3+}$	4.29	22

[a]Abbreviations used: en = ethane-1,2-diamine; tacn = 1,4,7-triazacyclononane; tame = 1,1,1-tris(aminomethyl)ethane; Me_3-tame = *N*,*N*′,*N*″-trimethyl-1,1,1-tris(aminomethyl)ethane.

basicity of the oxo bridge.[7−10] In Table 1, we have listed relevant data for selected dinuclear, oxo-bridged complexes of chromium(III). The variation of more than 10 orders of magnitude of the basicity of the oxo bridge and the 85% increase in the value J of upon changing the ligands from ammonia to methyl isocyanide is remarkable. Concerning the basicity of the oxo bridge, it should be noted that the charge of the cation cannot be the source of the variation of the acid strengths, because both the weakest acid (**1**) and the strongest acid (**11**) are the most positively charged (+5) cations, whereas the remaining ones have a positive charge of +3. It should furthermore be mentioned that the magnetic properties of **1**,[23] **8**,[8] and **10**,[12] in their protonated forms, have been investigated. The reported J values are in the range of 22−36 cm^{-1}. In this work, we present a model based on valence-bond-configuration interaction that explains the variation of more than 10 orders of magnitude for the basicity of the oxo bridge in the oxo-bridged dinuclear chromium(III) complexes and, in a consistent way, correlates this basicity with the antiferromagnetic coupling and with features in the optical absorption spectrum.

EXPERIMENTAL SECTION

Materials. $[Cr(NCCH_3)_4](BF_4)_2$, methyl isocyanide, and $[(bpy)_2(SCN)CrOCr(NCS)(bpy)_2](ClO_4)_2{\cdot}2H_2O$ (**8**$(ClO_4)_2{\cdot}2H_2O$) were synthesized according to literature methods.[24,25,9] Acetontrile and methanol was dried over molecular sieves. The reactions were carried out in standard Schlenk equipment, and solvents were purged with dinitrogen (N_2) prior to use.

Synthesis of $[(CH_3NC)_5CrOCr(CNCH_3)_5](PF_6)_4{\cdot}2CH_3CN$ (11$(PF_6)_4{\cdot}2CH_3CN$). Under a dinitrogen (N_2) atmosphere, $[Cr(NCCH_3)_4](BF_4)_2$ (2.0 g, 5.1 mmol) was placed in a Schlenk tube and CH_3NC (2.6 mL, 50 mmol) and CH_3CN (5 mL) was then added to afford a dark green solution. The solution was then exposed to the open atmosphere and air was bubbled through the solution for 30 min, during which the color of the solution changed to red-brown. Diethyl ether (40 mL) was then added dropwise under stirring and the resulting precipitate was filtered off, washed with diethyl ether, and dried in vacuo, yielding 2.2 g of a crude, brown product. For purification, a small portion (∼100 mg) was washed four times with CH_3OH to afford a red product. Single crystals were grown via the layering of a solution of the red product in CH_3CN with a concentrated solution of tetrabutylammonium hexafluorophosphate in CH_3CN. After 2 h, a small crop of the crystals of **11**$(PF_6)_4{\cdot}2CH_3CN$ suitable for X-ray crystallography could be isolated. ^1H NMR ([D_6]dmso): 2.08 (1H, s, CH_3CN), 3.19 (5.5H, t, CH_3NC). Anal. Calcd for $C_{21}H_{31.5}N_{10.5}Cr_2F_{24}OP_4$: C, 22.30; N, 13.01; H, 2.81. Found: C, 22.59; N, 12.80; H, 2.92.

X-ray Crystallography. Racemate crystals of **8**$(ClO_4)_2{\cdot}2H_2O$ (Δ,Δ/Λ,Λ) were grown by taking a small amount of reaction mixture, before boiling it, containing $[(bpy)_2Cr(OH)_2Cr(bpy)_2](ClO_4)_4$ and combining it with thiocyanate in water in a small closed vial in an oven at 60 °C. Small crystals formed overnight. Crystals of **8** and **11** were mounted, and intensity data were collected at 123(2) K on an Enraf-Nonius KappaCCD area detector, using ω and θ scans with a scan width of 1.0° and exposure times of 60 s, using the program COLLECT.[26] The crystal-to-detector distance was 35.0 mm. The program EVALCCD was used for data reduction, and the data were corrected for absorption by integration.[27] The structures were solved with direct methods utilizing SHELXS[28] and refined by least-squares methods using SHELXL97[29] for **11** and Olex2[30] for **8**. All non-hydrogen atoms were refined using anisotropic displacement parameters of 1.2U_{eq} of the

dx.doi.org/10.1021/ic4027927 | Inorg. Chem. 2014, 53, 2996−3003

parent atom, except for methyl and water hydrogens, which were constrained to $1.5U_{eq}$ of the parent atom. Crystallographic data are given in the Supporting Information (Table S-1).

Calculation of Exchange Coupling Constants. The J calculations were performed using the ORCA 2.7 program, as described earlier.[11] Although tempting, straightforward attempts at calculation of the pK_a values of the hydroxo-bridged compounds by density functional theory (DFT) were not fruitful.

RESULTS AND DISCUSSION

Syntheses. The reaction between the sky-blue complex $[Cr(NCCH_3)_4](BF_4)_2$ and a 10-fold excess of CH_3NC in a CH_3CN solution under a dinitrogen (N_2) atmosphere results in the immediate formation of a green complex, most likely the cation $[Cr(CNCH_3)_6]^{2+}$ (cf. the absorption spectrum in the Supporting Information). It is noteworthy that the chromium(II) ion apparently coordinates CH_3NC much more strongly than CH_3CN. However, this complex was not isolated in the solid state. The subsequent reaction between this complex and molecular dioxygen (O_2) results in the formation of the red complex $[(CH_3NC)_5CrOCr(CNCH_3)_5]^{4+}$ (**11**). This reaction is similar to the reaction between $[Cr(NCCH_3)_6]^{2+}$ and molecular dioxygen (O_2) in CH_3CN, which leads to the formation of the green complex $[(CH_3CN)_5CrOCr(NCCH_3)_5]^{4+}$ (**10**).[2] Elemental analysis of the bulk product suggested the stoichiometry **11**$(PF_6)_4\cdot 0.5CH_3CN$. In the case of the single crystals, having the stoichiometry **11**$(PF_6)_4\cdot 2CH_3CN$, the rapid loss of solvent CH_3CN from the crystals precluded satisfactory elemental analyses, and this may also be the explanation for the deviation from the expected ratio of 1:5 of the integrated intensities of the ^{1}H NMR spectra. Interestingly, addition of the strong acid HBF_4 (in diethyl ether) to a CH_3CN solution of **11** does not result in a color change. This contrasts the behavior of **10**, where a color change from green to red has been observed as a result of a protonation of the oxo bridge.[12] Accordingly, the oxo bridge in **11** is less basic than in **10**.

Crystal Structures. An ORTEP plot of **11** is shown in Figure 1. This complex has a linear $CrOCr^{4+}$ core with the CH_3NC ligands in an eclipsed conformation, which is a geometry also found in the analogous chromium complexes **1** (see ref 5) and **10** (see ref 2) and in $[(CH_3CN)_5MO(NCCH_3)_5]^{4+}$ (M = V,[31] Mo,[32] Re[33]). The Cr–O bond distance of 1.7712(5) Å is longer than that observed in **10** (1.7556(5) Å).[2] The *trans* influence of the oxo bridge has the consequence that the Cr–C9 (Cr–C_{trans}) distance of 2.101(3) Å, on average, is 0.016 Å longer than the four Cr–C_{cis} distances. This elongation is shorter than those found in the five complexes mentioned above, where elongations in the range of 0.040–0.105 Å have been observed. The Cr–C–N geometries are essentially linear. The C–N bond distance in the isocyanide groups is not significantly dependent on being *cis* or *trans* to the oxo bridge. This parallels the situation in the only structurally analogous molybdenum isocyanide complex $[(xyl\text{-}NC)_5MoOMo(CN\text{-}xyl)_5]^{2+}$ (xyl = 2,6-dimethylphenyl), where the internal bonding in the isocyanide ligands, similarly, is unaffected by their disposition (*cis* or *trans*) to the oxo bridge.[34] Conversely, the oxo bridge exhibits a pronounced *trans* influence (~0.08 Å) on the axial Mo–C bonds. It is also noteworthy that, for molybdenum, the dinuclear Mo(III) acetonitrile complex has been isolated,[32] but not the dinuclear Mo(III) isocyanide complex.[35]

Complex **8** has previously been synthesized,[10] but no crystal structure was reported. The crystal structure of **8** is shown in Figure 2. The most notable feature in this structure is the slight deviation from linearity of the $CrOCr^{4+}$ core, with the Cr–O–Cr angle being 169.46(15)°. This deviation must be ascribed to the π–π stacking of the bipyridine groups (vide infra). The Cr–O distances are 1.795(3) and 1.803(3) Å. The *trans* influence of the oxo bridge results in an elongation of the Cr–N_{trans} bond of 0.07 Å, on average.

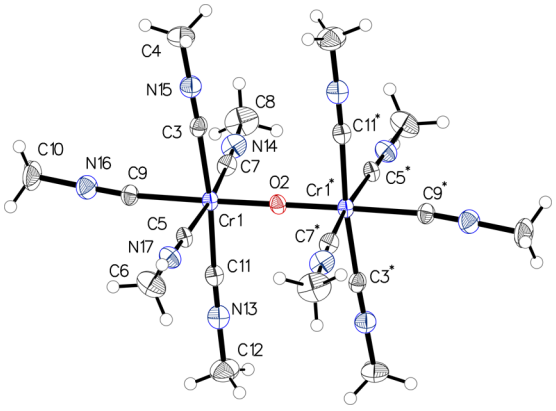

Figure 1. Molecular structure of **11**, showing 50% probability displacement ellipsoids. Important distances and angles: Cr1–O2, 1.7712(5) Å; Cr1–C3, 2.083(4) Å; Cr1–C5, 2.081(4) Å; Cr1–C7, 2.077(4) Å; Cr1–C9, 2.101(3) Å; Cr1–C11, 2.085(4) Å; Cr–O–Cr, 180°.

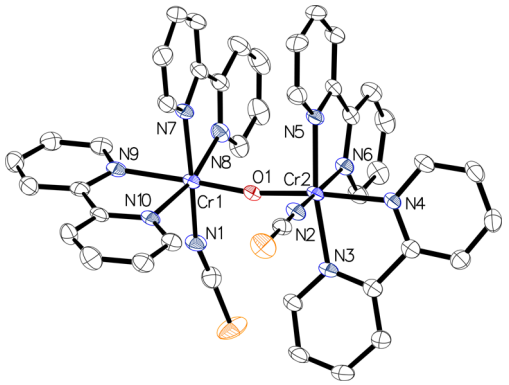

Figure 2. Molecular structure of the Δ,Δ isomer of **8**, showing 50% probability displacement ellipsoids. The H atoms have been removed for clarity. Important distances and angles: Cr2–O1, 1.795(3) Å; Cr1–O1, 1.803(3) Å; Cr2–N4, 2.126(4) Å; Cr1–N9, 2.122(4) Å; Cr2–N6, 2.076(3) Å; Cr2–N3, 2.065(3) Å; Cr2–N5, 2.049(3) Å; Cr1–N7, 2.085(3) Å; Cr1–N10, 2.061(3) Å; Cr1–N8, 2.073(3) Å; Cr2–N2, 2.017(3) Å; Cr1–N1, 2.013(3) Å; Cr1–O1–Cr2, 169.46(15)°.

Optical Absorption Spectra. The optical absorption spectrum of **11** is shown in Figure 3. For comparison, the spectra of **1** and **10** also are shown. All of the optical absorption data are listed in Table 3. The three spectra exhibit the same gross features, in which the absorption bands are shifted to lower energies upon going from **1** to **10** and further to **11**. The features have been assigned to ligand-field, pair-excitation, and charge-transfer transitions, as explained in the caption to Figure 3. The "e" band is a Cr ← O charge-transfer band and the observed reduction in transition energy (E_{CT}) through the series can explained by increasing nephelauxetism along the ligand series NH_3 < CH_3CN < CH_3NC. Furthermore, a higher

dx.doi.org/10.1021/ic4027927 | Inorg. Chem. 2014, 53, 2996–3003

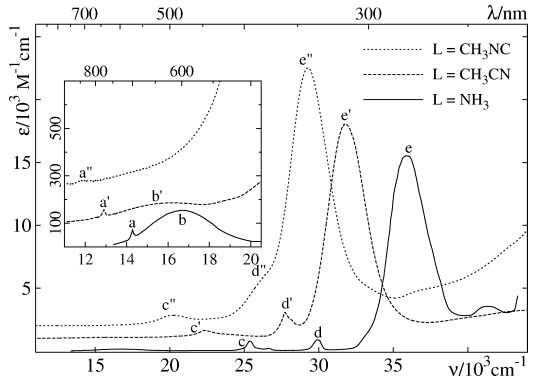

Figure 3. Optical absorption spectra of **1** (L = NH_3),[6] **10** (L = CH_3CN),[12] and **11** (L = CH_3NC) with data listed in Table 3. In accordance with previous assignments, the "a" bands are single excitations, the "b" bands correspond the first spin-allowed ligand field transition, the "c" and "d" bands are double excitations, and the "e" bands are charge-transfer bands. See text for details. The spectrum of **11** was measured in MeCN at room temperature.

Table 3. Electronic Transitions Referring to Figure 3 (ν, ε) in the Three $[L_5CrOCrL_5]^{4+}$ Complexes 1, 10, and 11[a]

	1 (L = NH_3)		**10** (L = CH_3CN)		**11** (L = CH_3NC)	
transition	ν (cm^{-1})	ε (M^{-1} cm^{-1})	ν (cm^{-1})	ε (M^{-1} cm^{-1})	ν (cm^{-1})	ε (M^{-1} cm^{-1})
a	14290	72	12900	57	11640	13
b	16800	154	16200	86		
c	25380	782	22300	640	20280	844
d	29950	880	27700	2080	~26000	~3700
e	36200	16000	31800	17000	29150	20400

[a]Data pertinent to **1** and **10** were taken from refs 6 and 12, respectively.

π acidity of the terminal ligands will lower the energy of the t_2 metal orbitals resulting in a lowering of the energy gap between the oxygen p-orbitals and the t_2 metal orbitals. In single-ion notation (O_h), the transition designated "a" corresponds to the transition $^2E_2,^4A_2 \leftarrow {}^4A_2,{}^4A_2$, a single excitation. Both terms originate from the t_2^3 electron configuration and, in the strong-field approximation theory, the energy difference is $9B + 3C$, where B and C are Racah parameters.[36] With this assignment, the average B value (assuming $C = 4.25B$) for the compounds **1**, **10**, and **11** is 598 cm^{-1}. Assuming the transitions labeled "b" provide Δ (vide supra), an average value for Δ can be approximately taken as 17 000 cm^{-1}. Using these values, a rough check on the strong field approximation, can be made. Indeed, diagonalization of the full LF matrices yield a cubic subconfiguration description of the ^2E state as $t_2^{2.97}e^{0.03}$ and in parallel $\partial[E(^2E) - E(^4A_2)]/\partial\Delta = 0.026$.[37] Experimentally, this energy varies by ~2600 cm^{-1} from 14 290 cm^{-1} in **1** to 11 640 cm^{-1} in **11**. This variation is, by far, too large to be explained by differences in the ligand field strength of the different ligands, given the very low sensitivity of this energy difference toward the octahedral ligand field splitting. Accordingly, it is explained by differences in nephelauxetism. Similarly, the double excitations designated with "c" (such as $^2E,^2E \leftarrow {}^4A_2,{}^4A_2$) and "d" (such as $^2T_2,^2E \leftarrow {}^4A_2,{}^4A_2$) in Figure 3 involve terms from the t_2^3 electron configuration.[6,38] Experimentally, these energies vary by ~5000 cm^{-1} and ~4000 cm^{-1} for "c" and "d", respectively. This is roughly twice the variation on the energy of the "a"-labeled transitions, which is consistent with the assignment of the "c" and "d" bands as double excitations. Notice that the energies of "c" is slightly less than twice the energy of "a", the reason being that the configurational mixing with the charge-transfer states of the double excitations is larger than that of the ground state.[39] The "b" feature corresponds to the single center transition $^4T_2(t_2^2e^1) \leftarrow {}^4A_2(t_2^3)$. Both terms originate from the free ion ^4F state, and in the strong-field approximation the energy of this transition is independent of the Racah parameters, which is consistent with the energy being approximately the same for **1** and **10**.

Calculation of the Exchange Coupling Constants. In compounds that are strongly coupled antiferromagnetically, the determination of the singlet−triplet energy gap (J), using magnetic susceptibility measurements, is very difficult at best, as the compounds are almost diamagnetic in the experimentally accessible temperature range, and it is therefore desirable to evaluate the coupling strength by other means. We have calculated the exchange coupling constant for **11** with broken symmetry DFT with a level of theory that has previously shown to give quantitatively accurate values for this particular type of dinuclear chromium(III) complexes.[11] Using this method and the experimental geometry determined by X-ray diffraction, we calculate the exchange coupling constant of **11** to be 825 cm^{-1}. In comparison, calculated values for **10** and **1**, are 685 and 441 cm^{-1}, respectively.[11] An alternative, computationally less costly, approach based on effective Hamiltonians parametrizing the LF and LMCT/MMCT function spaces was recently shown to provide almost equally good reproduction of experimental exchange couplings.[40] However, for the present fairly small dinuclear systems, brute force application of BS-DFT is both accurate and feasible. It should be noted that the exchange coupling constant is computed to be significantly larger for **11** than for **10** despite the larger Cr−O bond lengths in the former system, demonstrating the importance of the auxiliary ligand sphere in defining the coupling strength. Using an identical computational approach, the value for J in nonlinearly bridged **8** was based on the X-ray geometry and was determined to be 468 cm^{-1}, in good agreement with the experimentally determined value of 494 cm^{-1}.[10]

Bridge Basicity and Electronic Structure. In this section, we devise a model that semiquantitatively relates the variation in the optical absorption spectra and the variation in the antiferromagnetic exchange coupling constant to variations in the basicity of the oxo-bridge.

A discussion of absolute values of acid dissociation constants is inherently complicated by the rather large solvation energies pertinent to all involved species. Therefore, we would rather focus on the variation of the K_a values in Table 1 and the corresponding free-energy variation $\Delta G°$. The variation of $\Delta G°$ inferred from the values of K_a for **1** (K_{a1}) and **10** (K_{a10}) is obtained as

$$\Delta(\Delta G°) = -RT(\ln K_{a1} - \ln K_{a10}) \quad (2)$$

amounting to $\Delta(\Delta G°)$ = 59 kJ mol^{-1} at 298 K with K_{a1} and K_{a10} being $10^{-7.63}$ M and ~10^3 M (conservatively estimated lower bound on K_{a10}), respectively (see Table 1). For easy reference below, this corresponds to 4900 cm^{-1} per molecule.

This change in $\Delta G°$ is composed of a change in $\Delta H°$ and in $T\Delta S°$, i.e.,

$$\Delta(\Delta G°) = \Delta(\Delta H°) - T\Delta(\Delta S°) \quad (3)$$

dx.doi.org/10.1021/ic4027927 | Inorg. Chem. 2014, 53, 2996−3003

and, below, we argue that this change is mainly due to the enthalpy term $\Delta(\Delta H^\circ)$. We therefore neglect $\Delta(\Delta S^\circ)$, with the following justifications.

Accurate thermodynamic data pertinent to acid dissociation of a wide variety of organic acids were determined by Wynne-Jones.[41,42] For each class of acids, including organic carboxylic acids, as well as the first and second acid dissociation of amino acids, they found $T\Delta(\Delta S^\circ) < \Delta(\Delta H^\circ)$. With a comparable class of data, such as those relevant for the first acid dissociation of amino acids, typical values of $T\Delta(\Delta S^\circ) \approx 10$ kJ mol^{-1} (at 300 K) were found, which is significantly smaller than $\Delta(\Delta G^\circ)$ obtained above.

Detailed studies of acid dissociation constants involving dinuclear transition-metal complexes are not plentiful. Investigations by Spiccia and Marty[43] of the acidity of terminal water ligands in $[(H_2O)_5Cr(OH)Cr(OH_2)_5]^{5+}$ resulted in thermodynamic parameters for the first and second acid dissociation of $\Delta H^\circ = 47.6$ and 68.2 kJ mol^{-1}, respectively, and $\Delta S^\circ = 141$ and 147 J K^{-1} mol^{-1}, respectively. These data illustrate again that the variation in $T\Delta S^\circ$ is significantly smaller than the corresponding variation in ΔH°. Therefore, we confidently assume that $\Delta(\Delta G^\circ) \approx \Delta(\Delta H^\circ)$; furthermore, we approximate the enthalpy change with a reduction in the energy of the ground state of the oxo-bridged complex, relative to the ground state of the hydroxo-bridged, and this reduction in energy will now be interpreted using the valence-bond configuration interaction model.

In the framework of the valence-bond configuration interaction model,[44−46] the ground-state manifold of spin multiplets experiences a lowering and a splitting in energy, as a result of the interaction between the ground-state (GS) electron configuration and a ligand-to-metal charge transfer (LMCT) electron configuration, which, in turn, interacts with a metal-to-metal charge transfer (MMCT) electron configuration. In the following, the GS, LMCT, and MMCT electron configurations have the zeroth-order energy of 0, E_{CT}, and U, respectively. The hybridization one-electron matrix element between a metal d orbital and a ligand p orbital is designated V. In our specific situation, V describes the one-electron matrix element between a metal dπ orbital and a ligand pπ orbital, with π indicating the symmetry along the metal−ligand axis.

The energetic consequence of the GS-LMCT interaction is a spin-independent reduction in energy of all the ground-state manifold spin multiplets. This reduction in energy may be expressed as

$$E_1 = \frac{4V^2}{E_{CT}} \tag{4}$$

(see Figure 4). This expression quantifies, via second-order perturbation theory, the interaction via the two oxide pπ orbitals between the GS electron configuration $t_2^3(p\pi)^4t_2^3$ and the relevant terms from the charge-transfer configurations $t_2^4(p\pi)^3t_2^3$ and $t_2^3(p\pi)^3t_2^4$.[47] We notice that E_{CT} is an experimentally accessible parameter, see the intense bands in the region of 29 000−36 000 cm^{-1} in Figure 3 and Table 3; furthermore, the ratio V^2/E_{CT} may be identified as the angular overlap model parameter e_π pertinent to the chromium(III)-oxide bond. Glerup[6] has estimated $e_\pi \approx 4000$ cm^{-1} which is fairly consistent with the later[44] estimate of V being in the range of 10 000−11 000 cm^{-1}. V describes an interaction between the orbitals centered on different atoms and, consequently, the value depends strongly on the Cr−O bond distance (r). In the following, we model this dependence with an exponential as follows:

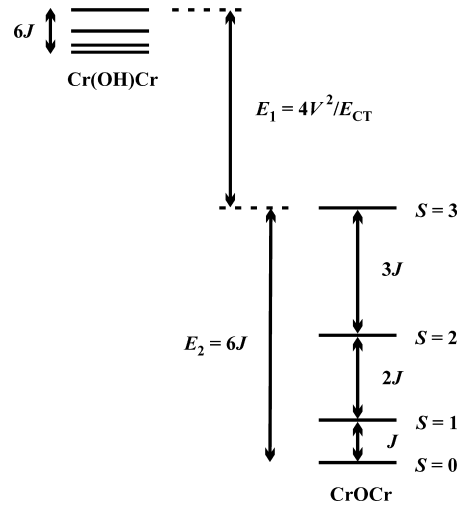

Figure 4. Graphical illustration of the small exchange splittings, $6J$, for the hydroxo-bridged complex in comparison with the relatively larger exchange splittings, J, for the oxo-bridged complex and of the reduction in the energy of the ground-state (GS) manifold of the oxo-bridged complex.

$$V = a\ \exp(br) \tag{5}$$

The Landé splitting of the GS manifold E_2 can be calculated using eq 6 from the experimental value of J (see Figure 4).

$$E_2 = 6J \tag{6}$$

In the absence of an experimental value of J, the value of J can be estimated by fourth-order in perturbation theory[48] to be

$$J = \frac{8}{9}\left(\frac{V^4}{E_{CT}^2}\right)\left(\frac{1}{E_{CT}} + \frac{1}{U}\right) \tag{7}$$

Combination of eqs 5 and 7 gives eq 8

$$J = \frac{8}{9}\frac{a^4}{E_{CT}^2}\left(\frac{1}{E_{CT}} + \frac{1}{U}\right)\exp(4br) = da^4\ \exp(4br) \tag{8}$$

with

$$d = \frac{8}{9}\left(\frac{1}{E_{CT}^2}\right)\left(\frac{1}{E_{CT}} + \frac{1}{U}\right)$$

The radial dependence of J for **1** and **10** was studied earlier,[11] using broken symmetry DFT (vide supra) and the calculated values of J were analyzed with the exponentials

$$J = c\ \exp(4br) \tag{9}$$

Herein, we have performed the same analysis on **11**, with the results (including the results for **1** and **10**) being collected in Figure 5. All three curves were modeled with eq 9 with the same exponent b (−1.24 Å^{-1}),[49] but with clearly different prefactors c varying by a factor of approximately $c(\mathbf{11})/c(\mathbf{1}) = 1.6$. The prefactor c obtained in this way can be modeled as follows: With E_{CT} taking the experimental values 29 150 and 36 200 cm^{-1} for **11** and **1**, respectively, and a constant U estimated[44] to be 90 000 cm^{-1}, we find the ratio $d(\mathbf{11})/d(\mathbf{1}) = 1.8$. Via combination of eqs 8 and 9, we obtain the correlation $c = da^4$. From the fact that the ratio $c(\mathbf{11})/c(\mathbf{1})$ is in good

dx.doi.org/10.1021/ic4027927 | Inorg. Chem. 2014, 53, 2996−3003

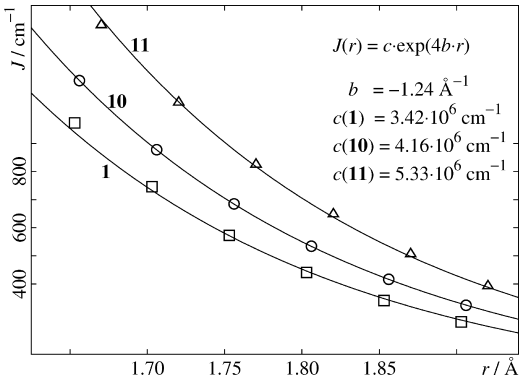

Figure 5. Theoretically computed values of J for 1 (□), 10 (○), and 11 (△) as function of the Cr−O bond distance (r). The curves straddeling the points are least-squares refinement of $J = c\exp(4br)$ to the r, $\ln(J)$ data.

agreement with the ratio $d(\mathbf{11})/d(\mathbf{1})$, the value of a can be approximated to be constant and estimated by eq 10 to be, on average, $a = 1.04(1) \times 10^5$ cm^{-1} in **1**, **10**, and **11**.

$$a = \sqrt[4]{\frac{9cE_{CT}^{\ 2}}{8\left(\frac{1}{E_{CT}} + \frac{1}{U}\right)}} \tag{10}$$

Hence, to the lowest-order in perturbation theory, the energy difference between the ground states of the hydroxo-bridged and oxo-bridged complex amounts to $E = E_1 + E_2$ and E can accordingly be calculated from eqs 4−7, using the parameters $a = 1.04 \times 10^5$ cm^{-1}, $b = -1.24$ Å^{-1}, and experimental values of at least two of the parameters r, E_{CT}, and J.[50] Now, we may assess the relative importance of E_1 and E_2. Using the average values of V, E_{CT}, and J (10 500, 33 000, and 600 cm^{-1}, respectively), we obtain $E_1 = 13\,360$ cm^{-1} and $E_2 = 3600$ cm^{-1}. Despite E_1 and E_2 being of the same order of magnitude, the total reduction in the energy of the $S = 0$ spin multiplet in the oxo-bridged complex, relative to the hydroxo-bridged complex, is dominated by E_1. Now, we can estimate, from the experimental data, the E_1 and E_2 values for each of **1** and **10**. Using eqs 4−7 and the values of E_{CT} being 36 200 and 31 800 cm^{-1}, we obtain E_1 values of 13 660 and 17 490 cm^{-1} and $E_2 = 2410$ and 4340 cm^{-1} for **1** and **10**, respectively. The sum of the changes in E_1 and E_2 in which the change in E_1 is the dominating factor, amounts to 5760 cm^{-1} corresponding to $\Delta(\Delta G°) = 68.9$ kJ mol^{-1} or $\Delta pK_a = 12.1$ ($T = 298$ K). Hence, we have justified the variation in the energy lowering of the ground state, as a result of a deprotonation of the hydroxobridge. Finally, we introduce an energy parameter E_o, which allows us to express the absolute value of $\Delta G°$:

$$\Delta G° = E_0 - E_1 - E_2 \tag{11}$$

where E_0 accounts for the differences in hydration energies of the involved species in eq 1 and the entropy term. This parameter is assumed the same for all the compounds. Therefore, the pK_a values may be obtained as

$$pK_a = \frac{E_0 - E_1 - E_2}{RT \ln 10} \tag{12}$$

where $E_0 = 235.8$ kJ mol^{-1} was chosen to fix $pK_a = 7.63$ for **1**, using the values of E_1 and E_2 mentioned above.

DISCUSSION

Using eq 12, the value of $pK_a = -4.4$ for protonated **10** is in accordance with our experimental finding that $pK_a < -2$. Similarly, it can be calculated that protonated **11** is more acidic (3.4 pK_a units) than protonated **10**, despite the fact that $r(\mathbf{11}) > r(\mathbf{10})$, which is also in qualitative agreement with our experimental findings. These results are presented in Figure 6,

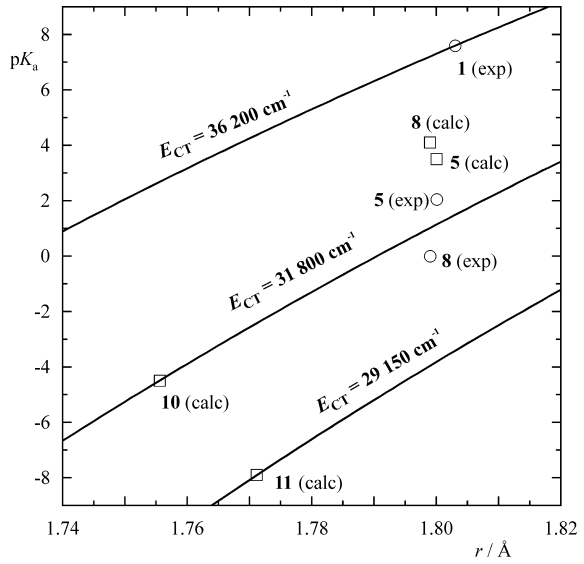

Figure 6. Values of pK_a, as a function of the Cr−O bond distance (r). The curves represent calculated values determined using eq 12, with the selected values $E_{CT} = 29\,150$, 31 800, and 36 200 cm^{-1} (the values of E_{CT} for **11**, **10**, and **1**) The points denoted by open squares (□) represent calculated values for **5**, **8**, **10**, and **11** and the points denoted by open circles (○) represent experimental values of **1**, **5**, and **8**.

where plots of pK_a vs r are displayed for values of E_{CT} found in **1**, **10**, and **11**. An additional plot of the results is shown in the Supporting Information. Values for E_{CT} for the complexes **2**−**9** are not listed in Table 1. Assignments of the bands in the UV range are difficult, because of the presence of intense intraligand transitions in the tpa, bpy, or phen ligands. An estimation of pK_a for protonated **2**−**9** requires accordingly experimental values of both r and J, which is the case only for **5** and **8**.[50] In these two cases, the value of E_2 can be obtained from the experimental value of J (being 510 and 494 cm^{-1}, respectively) and eq 6, whereas the value of E_{CT} needed to calculate E_1 in eq 4 can be obtained from J and eq 7. This gives the value of E_{CT} to be 33 330 and 33 790 cm^{-1} in **5** and **8**, respectively, from which the pK_a values can be calculated to be 3.6 and 4.1, respectively. The calculated values of pK_a are somewhat higher than the values determined experimentally, especially for **8**. This deviation may be explained in terms of energetically favorable $\pi-\pi$ stacking interactions in **2**−**9**. In the deprotonated forms, it has a linear Cr−O−Cr core; a stacking of parallel aromatic rings is found in the structures of **5** and **8** with an interplanar distance of ∼3.6 Å. This distance falls in the range typically found in $\pi-\pi$ stacking (3.3−3.8 Å).[51] In the protonated forms, having a bent Cr−O−Cr core, this stacking is more or less disrupted. With regard to the interaction energy, it should be mentioned that Sun recently[52] calculated an energy of 24 kJ mol^{-1} (corresponding to $\Delta pK_a = 4.2$) for the formation of a sandwich dimer of two parallel 2,2′-bipyridine molecules with an interplanar distance of 3.67 Å, which is close

dx.doi.org/10.1021/ic4027927 | Inorg. Chem. 2014, 53, 2996−3003

to the distance found in **7**. Furthermore, Sherrill[53] calculated an energy of 6.5 kJ for the formation a sandwich dimer of two parallel pyridine molecules separated by 3.8 Å. It should be noted that, in tpa complexes **2**−**7**, there are two such interactions per molecule. In summary, $\pi-\pi$ stacking interactions in the deprotonated forms could explain the higher acidity of protonated **2**−**9** than that predicted from eq 12. The pK_a values for the complexes **2**−**7** fall in the range of 0.64−4.25 and depend accordingly on the nature of the terminally coordinated, anionic ligand. Holwerda discussed this observation earlier, and he noted, in accordance with our model, that higher π acidity of the anionic ligand leads to lower pK_a values.[7] The energy of the $^4T_2 \leftarrow {}^4A_2$ transition of the hydroxo-bridged complex was used as an experimentally available measure of the π acidity. However, this, in our view, is somewhat misleading, since this transition energy, which is equal to the ligand-field parameter Δ, also depends on the σ donor properties of the ligand (in angular overlap parameters: $\Delta = 3e_\sigma - 4e_\pi$). Instead, the value of E_{CT} should be used as a measure of the π acidity of the ligands as described above. Holwerda also used the value of J as a measure of the π bonding in the CrOCr core and thereby obtained a correlation between J and pK_a.[8] In our model, J and pK_a are inherently correlated in the way that the Landé splitting $E_2 = 6J$ is but one of two contributions to the reduction in the energy of the $S = 0$ state in the GS manifold.

CONCLUSIONS

A new, dinuclear oxo-bridged chromium(III) complex (**11**) has been prepared employing the strong π-acidic methyl isocyanide as a homoleptic auxiliary ligand. This complex exhibits the greatest antiferromagnetic coupling observed thus far for such systems. From computational modeling in conjunction with spectroscopic data, a pronounced dependence of coupling strength on the auxiliary ligand sphere was inferred for oxo-bridged dichromium(III) systems. This implies that electronic properties of nonbridging ligands, which are not directly involved in exchange pathways, can have profound importance for magnetic couplings and provides a strong case for design in magnetochemistry.

We have presented a model that explains the intriguing, >10-orders-of-magnitude variation of the acid dissociation constant of the hydroxo bridge in the dinuclear chromium(III) complexes, in terms of differences in the reduction in energies, in addition to the Landé splitting of the ground-state manifold. This model requires only experimental data for two of the following parameters: Cr−O distance (r), energy of the Cr ← O charge-transfer band (E_{CT}), and triplet energy (J). Based on the present model, and in contrast with previous attempts at rationalizing these properties, it is concluded that the reduction in energy of all spin states by configuration interaction between the ground state and ligand-to-metal charge transfer (LMCT) states dominates the influence of electronic structure on the bridge basicity in these oxo-bridged dinuclear systems.

ASSOCIATED CONTENT

Supporting Information

Crystallographic data for **8**$(ClO_4)_2 \cdot 2H_2O$ and **11**$(PF_6)_4 \cdot 2CH_3CN$ (Table S1), optical absorption spectrum of $[Cr(CNCH_3)_6]^{2+}$ (Figure S1), and a contour plot of pK_a vs (r, E_{CT}) (Figure S2). Crystallographic data and CIF files are also provided. This material is available free of charge via the Internet at http://pubs.acs.org. The crystallographic data have been deposited at Cambridge Structural Database (www.ccdc.cam.ac.uk) (CCDC Nos. 937993 and 937994 for **8**$(ClO_4)_2 \cdot 2H_2O$ and **11**$(PF_6)_4 \cdot 2CH_3CN$, respectively).

AUTHOR INFORMATION

Corresponding Author

*E-mail: dossing@chem.ku.dk.

Notes

The authors declare no competing financial interest.

REFERENCES

(1) Jørgensen, S. M. *J. Prakt. Chem.* **1882**, *25*, 321−346.
(2) Barra, A.-L.; Døssing, A.; Morsing, T.; Vibenholt, J. *Inorg. Chim. Acta* **2011**, *373*, 266−269.
(3) Pedersen, E. *Acta Chem. Scand.* **1972**, *26*, 333−342.
(4) Schwarzenbach, G.; Magyar, B. *Helv. Chim. Acta* **1962**, *45*, 1425−1453.
(5) Urushiyama, A. *Bull. Chem. Soc. Jpn.* **1972**, *45*, 2406−2412.
(6) Glerup, J. *Acta Chem. Scand.* **1972**, *26*, 3775−3787.
(7) Gafford, B. G.; O'Rear, C.; Zhang, J. H.; O'Connor, C. J.; Holwerda, R. A. *Inorg. Chem.* **1989**, *28*, 1720−1726.
(8) Tekut, T. F.; O'Connor, C. J.; Holwerda, R. A. *Inorg. Chem.* **1993**, *32*, 324−328.
(9) Gafford, B. G.; Holwerda, R. A.; Schugar, H. J.; Potenza, J. A. *Inorg. Chem.* **1988**, *27*, 1126−1128.
(10) Holwerda, R. A.; Tekut, T. F.; Gafford, B. G.; Zhang, J. H.; O'Connor, C. J. *J. Chem. Soc., Dalton Trans.* **1991**, 1051−1055.
(11) Morsing, T. J.; Sauer, S. P. A.; Weihe, H.; Bendix, J.; Døssing, A. *Inorg. Chim. Acta* **2013**, *396*, 72−77.
(12) Andersen, N. H.; Døssing, A.; Mølgaard, A. *Inorg. Chem.* **2003**, *42*, 6050−6055.
(13) Semenaka, V. V.; Nesterova, O. V.; Kokozay, V. N.; Dyakonenko, V. V.; Zubatyuk, R. I.; Shishkin, O. V.; Boča, R.; Jezierska, J.; Ozarowski, A. *Inorg. Chem.* **2010**, *49*, 5460−5471.
(14) Mønsted, L.; Mønsted, O.; Springborg, J. *Inorg. Chem.* **1985**, *24*, 3496−3498.
(15) Mønsted, L.; Mønsted, O. *Acta Chem. Scand.* **1976**, *A30*, 203−208.
(16) Inskeep, R. G.; Bjerrum, J. *Acta Chem. Scand.* **1961**, *15*, 62−68.
(17) Andersen, P.; Døssing, A.; Glerup, J.; Rude, M. *Acta Chem. Scand.* **1990**, *44*, 346−352.
(18) Rude, M. Master's Thesis, University of Copenhagen, Copenhagen, Denmark, 1990.
(19) Andersen, P.; Matsui, H.; Nielsen, K. M.; Nygaard, A. S. *Acta Chem. Scand.* **1994**, *48*, 542−547.
(20) Døssing, A. Ph.D. Thesis, University of Copenhagen, Copenhagen, Denmark, 1990.
(21) Andersen, P.; Nielsen, K. M.; Pretzmann, U. *Acta Chem. Scand.* **1997**, *51*, 815−821.
(22) Stünzi, H.; Marty, W. *Inorg. Chem.* **1983**, *22*, 2145−2150.
(23) Glerup, J.; Weihe, H. *Inorg. Chem.* **1997**, *36*, 2816−2819.
(24) Henriques, R. T.; Herdtweck, E.; Kühn, F. E.; Lopes, A. D.; Mink, J.; Romao, C. C. *J. Chem. Soc., Dalton Trans.* **1998**, 1293−1297.
(25) Schuster, R. E.; Scott, J. E.; Casanova, J. *Org. Synth.* **1973**, *5*, 772.
(26) *COLLECT*; Nonius BV: Delft, The Netherlands, 1999.
(27) Duisenberg, A. J. M.; Kroon-Batenburg, L. M. J.; Schreurs, A. M. M. *J. Appl. Crystallogr.* **2003**, *36*, 220−229.
(28) Sheldrick, G. M. *Acta Crystallogr., Sect. A: Found. Crystallogr.* **1990**, *46*, 467−473.
(29) Sheldrick, G. M. *Acta Crystallogr., Sect. A: Found. Crystallogr.* **2008**, *64*, 112−122.
(30) Dolomanov, O. V.; Bourhis, L. J.; Gildea, R. J.; Howard, J. A. K.; Puschmann, H. *J. Appl. Crystallogr.* **2009**, *42*, 339−341.
(31) Cissell, J. A.; Kauer, N.; Nellutla, S.; Dalal, N. S.; Vaid, T. P. *Inorg. Chem.* **2007**, *46*, 9672−9677.
(32) McGilligan, B. S.; Wright, T. C.; Wilkinson, G.; Motevalli, M.; Hursthouse, M. B. *J. Chem. Soc., Dalton Trans.* **1988**, 1737−1742.

(33) Bera, J. K.; Schelter, E. J.; Patra, S. K.; Bacsa, J.; Dunbar, K. R. *Dalton Trans.* **2006**, 4011−4019.
(34) Igoshi, T.; Tanase, T.; Yamamoto, Y. *J. Organomet. Chem.* **1995**, *494*, 37−42.
(35) For molybdenum, a divalent dinuclear, $[(xyl\text{-}NC)_5MoOMo(CN\text{-}xyl)_5]^{2+}$ (ref 34), and a tetravalent mononuclear oxo-isocyanide system (e.g., *trans*-$[Mo(O)Cl(CNCH_3)_4]^{+}$) have been accessed. See, for example: Lam, C. T.; Lewis, D. L.; Lippard, S. J. *Inorg. Chem.* **1976**, *15*, 989−991.
(36) Lever, A. B. P. In *Inorganic Electronic Spectroscopy*; Elsevier: Amsterdam, 1968; p 182.
(37) Bendix, J.; Brorson, M.; Schaffer, C. E. *Inorg. Chem.* **1993**, *32*, 2838−2849.
(38) Güdel, H. U.; Dubicki, L. *Chem. Phys.* **1974**, *6*, 272−281.
(39) Schenker, R.; Weihe, H.; Güdel, H. U. *Inorg. Chem.* **1999**, *38*, 5593−5601.
(40) Tchougréeff, A. L.; Dronskowski, R. *J. Phys. Chem. A* **2013**, *117*, 7980−7988.
(41) Wynne-Jones, W. F. K. *Proc. R. Soc. London* **1933**, *A140*, 440−451.
(42) Everett, D. H.; Wynne-Jones, W. F. K. *Proc. R. Soc. London* **1941**, *A177*, 499−516.
(43) Spiccia, L.; Marty, W. *Polyhedron* **1991**, *10*, 619−628.
(44) Brunold, T.; Gamelin, D. R.; Solomon, E. I. *J. Am. Chem. Soc.* **2000**, *122*, 8511−8523.
(45) Tuczek, F.; Solomon, E. I. *Coord. Chem. Rev.* **2001**, *219−221*, 1075−1112.
(46) Tuczek, F.; Solomon, E. I. In *Comprehensive Coordination Chemistry II*, Vol. 2; Lever, A. B. P., Ed.; Elsevier: Amsterdam, 2003; pp 541−557.
(47) As pointed out by one referee, E_1 is the additional reduction in energy of the ground state upon removal of the proton in the hydroxo-bridged species.
(48) Weihe, H.; Güdel, H. U.; Toftlund, H. *Inorg. Chem.* **2000**, *39*, 1351−1362.
(49) There is a typographical error in the reported values of 4*b* in ref 11. The values of 4*b*, calculated in the range of r = 1.50−2.10 Å, should have been reported as −5.032 and −5.035 $Å^{-1}$ for **10** and **1**, respectively. These values are seen to differ slightly from the average value of 4*b* in **1**, **10**, and **11** found in this work (4*b* = −4.96 $Å^{-1}$). The reason for this deviation is that the present calculations include a smaller range of r (1.65−1.93 Å).
(50) Equation 8 correlates the parameters r, E_{CT}, and J. Accordingly, experimental values of only two of the parameters are necessary to calculate pK_a using eqs 4−6 and eq 12.
(51) Janiak, C. *J. Chem. Soc., Dalton Trans.* **2000**, 3885−3896.
(52) Mottishaw, J. D.; Sun, H. *J. Phys. Chem. A.* **2013**, *117*, 7970−7979.
(53) Hohenstein, E. G.; Sherrill, C. D. *J. Phys. Chem. A* **2009**, *113*, 878−886.